Carbon 123 (2017) 259–272

Contents lists available at ScienceDirect

Carbon

journal homepage: www.elsevier.com/locate/carbon

Carbon-coated sepiolite clay fibers with acid pre-treatment as low-cost organic adsorbents

Xueping Wu [a, *], Qingxin Zhang [a], Cun Liu [a], Xianlong Zhang [a], D.D.L. Chung [b, **]

[a] School of Chemistry and Chemical Engineering, Hefei University of Technology, Hefei 230009, China
[b] Composite Materials Research Laboratory, Department of Mechanical and Aerospace Engineering, University at Buffalo, The State University of New York, Buffalo, NY 14260-4400, USA

ARTICLE INFO

Article history:
Received 20 April 2017
Received in revised form
17 July 2017
Accepted 18 July 2017
Available online 19 July 2017

ABSTRACT

Carbon-nanoparticle-coated sepiolite hydrous-magnesium-silicate clay fibers are prepared by 220°C-autoclave hydrothermal carbonization of cellulose using 1.2-mol/L-hydrochloric-acid-pretreated sepiolite fibers. The deposited amorphous carbon nanoparticles (30–150 nm) nonuniformly and partially covering the sepiolite surface have surface functional groups (–CH_2, –CH_3, C=C and C=O), which enhance the organophilicity. Compared to a mixture of pristine sepiolite and hydrothermal carbon prepared without sepiolite, the carbon-coated sepiolite exhibits lower specific surface area but greater organic adsorption, due to the smaller pore size and particle size of the hydrothermal carbon coating compared to the hydrothermal carbon prepared without sepiolite. The acid pre-treatment decreases the sepiolite crystallinity and increases the deposited carbon content from 24.67 to 31.63 vol%, while increasing the specific surface area from 26.53 to 33.98 m^2/g, increasing the fraction of phenol removed from 47.1% to 57.1%, and increasing the monolayer phenol adsorption capacity from 4.1 to 5.26 mg/g. Compared to the acid treated but uncoated sepiolite, the carbon coating decreases the density from 2.227 to 1.696 g/cm^3 and decreases the specific surface area from 118 to 34 m^2/g, but increases the fraction of phenol removed from 6.1% to 57.1%. The acid pre-treatment gives greater adsorption than the addition of acid to the hydrothermal process liquid.

1. Introduction

Due to the rapid industrial growth, pollutant emission has been increasing. Among the organic pollutants, phenol, methylene blue and their derivatives are representatives, due to their large amounts in industrial wastewater and their high toxicity, even at very low concentrations [1]. Various methods have been employed to improve the efficiency and reduce the cost of organic substance removal, including adsorption, catalytic oxidation and Fenton and Fenton-like processes [2–6]. Adsorption is one of the simplest and most cost-effective methods of substance removal, due to its low cost and operational convenience. It is especially effective for the removal of organic pollutants (such as phenol) that do not degrade easily [7]. Among numerous adsorbents, activated carbons are superior for the removal of organic substances as a result of their high specific surface area, well-controlled porosity and excellent adsorption properties [8]. To obtain activated carbons, physical and chemical activation are the two main methods. For example, biomass-derived activated carbons are prepared using a two-step process consisting of carbonization and subsequent activation. Both steps require high temperatures and are thus expensive [9]. The development of low-cost adsorbents is critically needed.

Clays are natural low-cost adsorbents, due to their abundance in nature. Sepiolite is a type of clay in the form of a magnesium silicate hydrate. It naturally occurs as a fibrous clay mineral with chemical formula $Si_{12}O_{30}Mg_8(OH)_4(H_2O)_4 \cdot 8H_2O$ and an orthorhombic unit cell [10]. It is a phyllosilicate with a structure consisting of two layers of discontinuous tetrahedral silica sheet sandwiching a central magnesium oxide-hydroxide layer, with abundant silanol groups (Si–OH) located at the external surface [11]. From a microstructural viewpoint, sepiolite consists of alternating blocks and channels that are aligned in the fiber direction [12]. This

* Corresponding author.
** Corresponding author.
E-mail addresses: xuepingw@ustc.edu.cn (X. Wu), ddlchung@buffalo.edu (D.D.L. Chung).
URL: http://alum.mit/edu/www/ddlchung

http://dx.doi.org/10.1016/j.carbon.2017.07.063
0008-6223/

structure results in a unique multi-channel fibrous morphology. The cross-section of each channel along the length of the fibers is about 0.37 nm × 1.06 nm in size [12]. The sepiolite fiber length and width vary among deposits. The length is usually 2–10 μm and the width is usually 10–30 nm [13]. The nanoscale fibrous morphology makes sepiolite attractive for adsorption, due to the channels between the fibers and the substantially high specific surface area. However, the adsorption capacity of unmodified sepiolite for organic substances tends to be low [14]. Thus, various methods have been applied to functionalize sepiolite in order to enhance the adsorption; examples include acid treatment [15], heat treatment [16,17] and surfactant modification [10,18].

Among the abovementioned methods of modification of sepiolite, acid treatment is most commonly used for increasing the surface area and surface activity and reducing the amount of the impurities in the clay minerals [11,19,20]. The increase of the surface area and surface activity is due to the release of cations (Mg^{2+}, Al^{3+} and Fe^{3+}) from the octahedral sheet and the reduction of the amount of mineral impurities [16,21]. Moreover, the octahedral cations (Mg^{2+}, Al^{3+} and Fe^{3+}) are substituted by hydrogen ions when the acid penetrates the channels and results in the formation of two silanol groups. The silanol groups are active sites for biopolymers due to hydrogen bonding, thereby providing the needed surface modification [12,22,23]. Another route involves polymer-matrix composites [12]. The composite fabrication can be facilitated by the interaction of the silanol groups on the sepiolite surface with the hydroxyl groups of the polymer matrix [23,24]. Another method of surface modification involves the coating of the clay mineral surface with carbon, which is attractive for its surface functional groups and its organophilicity [25,26]. Due to its inherent solid-state acidity, diatomite (powder from a soft, siliceous sedimentary rock) plays a catalytic role in the coating of the diatomite with carbon by a vapor-deposition polymerization process that uses furfuryl alcohol as the carbon precursor [26]. Due to the slow polymerization of furfuryl alcohol and the introduction of phosphoric-acid impregnated mesostructured silica, carbon is formed in the mineral pores [27]. Single-walled carbon nanotubes have been grown on sepiolite by chemical vapor deposition, using the sepiolite as both a catalyst and a catalyst support [10].

A multi-adsorbent system can also be prepared by physically mixing two adsorbents, such as dolomite and tea waste [28]. Compared to the adsorption capacity of tea waste (130.5 mg/g) and dolomite (113.3 mg/g) for methylene blue, the adsorption capacity of the mixture of tea waste and dolomite is higher, reaching 150.4 mg/g. However, Albadarin et al. [28] did not compare the adsorption capacity of the multi-adsorbent system in the form of a mixture with the corresponding multi-adsorbent system in the form of one adsorbent coating the other adsorbent. Furthermore, the effect of acid pre-treatment of clay minerals on the subsequent coating of the clay minerals with carbon and on the adsorption capacity of the resulting multi-adsorbent system has not been previously reported. In the prior work of some of the authors, carbon-coated clays, namely carbon-coated palygorskite and carbon-coated halloysite, were prepared by hydrothermal carbonization for the improvement of the phenol adsorption capacity of the clays [25,29–31]. As mentioned above, the silanol groups of clay minerals are the active sites for the interactions with biopolymers, such as cellulose, chitosan and glucose [12]. However, the concentrations of these groups are low, thus resulting in a small amount of deposited carbon on the clay. The low carbon content in turn results in a low phenol adsorption capacity. The density of the silanol groups differs among clay minerals. In particular, the density of the silanol groups of fibrous clays (sepiolite and palygorskite) is much higher (ca. 2 Si–OH groups/nm^2) than that of lamellar clays [12]. No prior work has provided a comparison of sepiolite and palygorskite in this regard. In this work, we conducted the phenol adsorption on carbon-coated sepiolite and obtained the removal rate of 47.1%. The value is higher than the previously reported corresponding value of 33.0% for carbon-coated palygorskite [32].

The acid treatment is expected to increase the concentration of the silanol groups on the sepiolite, due to the bond breaking at the octahedral sites, of which there are eight per sepiolite formula unit. In contrast, there are only five in palygorskite [33]. During the acid treatment, the removal of the Mg^{2+} and Fe^{3+} ions is easier than that of the Al^{3+} ions. This is because the Al^{3+} ions occupy the center of the silicate ribbons and, thus, cannot be removed easily [34]. A mild acid treatment is sufficient to remove most of the octahedral cations in sepiolite, which has a relatively high magnesium content. The ion removal causes increase in the specific surface area [21].

In this study, the sepiolite is used as a carrier for directing carbon growth during hydrothermal carbonization using cellulose as the carbon source. The novel part of this study pertains to the effects of acid treatment of the sepiolite on the subsequent hydrothermal carbonization of cellulose and concomitant deposition of carbon on the sepiolite, and on the ability of the sepiolite to adsorb organic substances.

The scientific objectives of this paper are (i) investigating the effect of acid pre-treatment on the hydrothermal deposition of carbon on the sepiolite and on the morphology and amount of the deposited carbon, using cellulose as the carbon source, (ii) investigating the effect of the acid pre-treatment on the ability of carbon-coated sepiolite to serve as an adsorbent of organic substances, particularly phenol and methylene blue, (iii) studying the characteristics of the abovementioned adsorption, (iv) comparing the organic adsorption removal rate for carbon-coated sepiolite and the corresponding mixture of hydrothermal carbon and sepiolite, and (v) comparing the organic adsorption removal rate for carbon-coated sepiolite obtained from acid-pretreated sepiolite with that for carbon-coated sepiolite obtained from hydrocarbon deposition on sepiolite without acid pretreatment but in the presence of the acid added to the hydrothermal process liquid.

2. Materials and methods

2.1. Raw materials

The pristine sepiolite acquired from Nanyang, China, was ground and 200-mesh sieved. Its chemical composition was 38.27 wt.% SiO_2, 22.48 wt.% MgO, 20.14 wt.% CaO, 0.86 wt.% Al_2O_3, 0.28 wt.% Fe_2O_3, 0.12 wt.% K_2O, 0.11 wt.% NaO and 17.74 wt.% others. Microcrystalline cellulose (powder), phenol, methylene blue (MB), hydrochloric acid (HCl) and ammonium ferrous sulfate hexahydrate ($FeSO_4(NH_4)_2SO_4 \cdot 6H_2O$) were all of analytical grade, as purchased from Sinopharm Chemical Reagent (Shanghai) Co. Ltd., and used as received without further purification. Ammonium ferrous sulfate hexahydrate was used as the catalyst, as in prior work [25,30,31].

2.2. Acid pre-treatment of sepiolite

Sepiolite (4.0 g) was immersed in 50.0 mL of hydrochloric acid aqueous solutions (concentration 0.3, 0.6, 1.0, 1.2 and 2.0 mol/L) at room temperature, and then stirred for 1.0 h. Subsequently the solid was separated from the suspensions by using a centrifuge and then washed with distilled water until it became neutral (pH = 7). The obtained material was dried at 60 °C overnight. These samples were designated "*x*SEP", where *x* stands for the hydrochloric acid concentration in mol/L. The pristine sepiolite, designated "SEP", was also studied for the sake of comparison.

2.3. Hydrothermal deposition of carbon on sepiolite

2.3.1. Hydrothermal deposition of carbon on acid-pretreated sepiolite

Dried sepiolite powder (2.0 g) was immersed in distilled water (70.0 mL). The mixture was stirred for 0.5 h at room temperature to disperse the sepiolite. Cellulose (4.0 g) was then introduced, followed by stirring for 1.0 h. Then, ammonium ferrous sulfate hexahydrate (0.5 wt.%) was added to the suspension to serve as the catalyst and then the suspension was stirred for 0.5 h. The final suspension was transferred to a Teflon-lined stainless steel autoclave (100 mL in total inner volume) filled to 80 vol% of the capacity, sealed, and maintained at 220 °C for 48.0 h. The carbonized products were subsequently filtered, washed with distilled water and ethanol several times until they became neutral (pH = 7), and then dried at 60 °C to achieve a constant weight. These samples were designated "*y*SEP/C", where *y* is the concentration of hydrochloric acid. The absence of *y* in the designation means that no acid treatment was conducted. For example, 1.2SEP/C refers to the carbon-coated sepiolite obtained from the hydrothermal deposition of carbon on acid pre-treated sepiolite, such that the acid concentration used in the acid pre-treatment is 1.2 mol/L.

2.3.2. Hydrothermal deposition of carbon on sepiolite without acid pre-treatment but in the presence of acid

For comparison, 2.0 g of pristine sepiolite was immersed in 25 mL of 1.2 mol/L hydrochloric acid and stirred for 1.0 h. The proportion of sepiolite to hydrochloric acid solution is the same as that for the acid pre-treatment of the sepiolite described in Sec. 2.2. Then 4.0 g of cellulose with 55 mL of distilled water was introduced and stirred under the same condition. Then the ammonium ferrous sulfate hexahydrate (0.5 wt.%) was added to the suspension. After stirring for 0.5 h, the suspension was transferred to a Teflon-lined stainless steel autoclave and maintained there at 220 °C for 48.0 h. The abbreviation 1.2-SEP/C refers to the carbon-coated sepiolite prepared by the one-step hydrothermal process of the sepiolite without the acid pre-treatment but with 1.2 mol/L hydrochloric acid added to the process liquid.

2.4. Hydrothermal formation of carbon in the absence of sepiolite

Under the same condition as for the hydrothermal deposition of carbon on the acid-pretreated sepiolite (Sec. 2.2), cellulose was hydrothermally treated in the absence of sepiolite, but still in the presence of ammonium ferrous sulfate hexahydrate, in order to obtain carbon in the absence of the sepiolite for the sake of comparison. The resulting hydrothermal carbon is designated "HC".

2.5. Mixtures of sepiolite and hydrothermal carbon

Dry mixtures of sepiolite and hydrothermal carbon HC were prepared by mixing sepiolite and HC at predetermined weight proportions for the purpose of comparison with the behavior of sepiolite with hydrothermal carbon deposition (coating). The mixing was conducted by manual shaking in a conical flask for 5 min without stirring. For evaluating the organic adsorption behavior of the mixtures, dispersions of sepiolite and HC (at predetermined weight proportions) in either phenol or methylene blue were prepared by agitating the dispersion using a water-filled shaking bath.

The mixtures/dispersions are designated SEP + HC and 1.2SEP + HC for the sepiolite without and with the acid pre-treatment, respectively. The 1.2 in the designation indicates that the acid concentration in the pre-treatment is 1.2 mol/L. The mixing ratio is based on the ratio of the sepiolite and carbon in the corresponding carbon-coated sepiolite. For example, the carbon volume fraction of the mixture SEP + HC is the same as that of SEP/C, as calculated by using the Rule of Mixtures [35]. More information on the calculation of the carbon volume fraction is given in Sec. 2.7.

2.6. Characterization methods

Fourier-transform infrared (FTIR) spectroscopy was conducted using a Fourier-transform infrared spectrometer (ThermoNicolet 67, Madison, U.S.A) in the wavenumber range from 400 cm^{-1}–4000 cm^{-1} using potassium bromide (KBr) pellets mixed with the specimen. Powder X-ray diffraction (XRD) was performed using an X-ray diffractometer with a copper anode operating at 40 kV and 100 mA (D/MAX2500V, Rigaku, Japan). The nitrogen gas (N_2) adsorption-desorption isotherms were obtained at 77 K (Nova 2200e, Quantachrome, U.S.A). The samples were outgassed at 150 °C for 6 h at a pressure of 10^{-6} mm Hg before analysis. The specific surfaces area was calculated by using the Brunauer–Emmett–Teller (BET) equation. The pore size distribution was obtained using the Barrett–Johner–Halendar (BJH) method. The morphologies and sizes of the products were observed using a JEOL JSM-6700 F field-emission scanning election microscope (SEM). Transmission electron microscope (TEM) images were obtained using a JEM-2100 F instrument equipped with an energy dispersive X-ray spectrometer (EDX). The particle size distribution of HC was obtained from several randomly selected areas in the TEM images, with each area containing about 300–400 particles. Elemental analysis (EA) was conducted using an elemental analyzer (for CHNS + O analysis, purge-and-trap gas chromatography, vario EL cube, Elementar, Germany).

2.7. Analysis based on the Rule of Mixtures

The volume fractions of carbon (V_f) and sepiolite (1 - V_f) in the carbon-coated sepiolite were calculated by using the Rule of Mixtures [35], i.e.,

$$\rho_1 = (1\text{-}V_f)\,\rho_2 + V_f \cdot \rho_3, \tag{1}$$

where ρ_1 (g/cm^3) is the true density of the carbon-coated sepiolite; ρ_2 (g/cm^3) is the true density of the uncoated sepiolite with the corresponding extent of acid pre-treatment; ρ_3 (g/cm^3) is the true density of HC. The true densities were measured by pycnometry.

In order to obtain more information on the distinction between the carbon coating on the sepiolite and HC, the values of the specific surface area and phenol removal rate of the carbon-coated sepiolite were calculated using the corresponding properties of the HC and uncoated sepiolite (with the corresponding extent of acid pre-treatment), based on the Rule of Mixtures, i.e.,

$$S_1 = (1-V_f)\,S_2 + V_f \cdot S_3 \tag{2}$$

$$\eta_1 = (1-V_f)\,\eta_2 + V_f \cdot \eta_3 \tag{3}$$

In Eq. (2), S_1 (m^2/g) is the calculated specific surface area of the carbon-coated sepiolite; S_2 (m^2/g) is the specific surface area of the uncoated sepiolite with the corresponding extent of acid pre-treatment; S_3 (m^2/g) is the specific surface area of HC. In Eq. (3), η_1 is the calculated organic removal rate of the carbon-coated sepiolite; η_2 is the organic removal rate of the uncoated sepiolite with the corresponding extent of acid pre-treatment; η_3 is the organic removal rate of HC.

2.8. Adsorption studies

Phenol adsorption studies were conducted using a 250.0 mL conical flask. An amount of 1.0 g of each adsorbent was added to the flask filled with 100 mL phenol solution of concentration ranging from 5.0 to 200.0 mg/L. Then, the flask was agitated in a shaker bath at 25 °C and a shaking speed of 200 rev/min for 120 min in order to reach the adsorption equilibrium. Subsequently the sample was centrifuged at 8000 rev/min for 1.0 min.

Similarly, the methylene blue adsorption studies were conducted under the same conditions with an adsorbent dose of 1 g/L. The concentration of the methylene blue solution ranged from 50.0 to 250.0 mg/L.

The phenol and methylene blue concentrations of the filtrates were measured with an ultraviolet-visible spectrophotometer (UV2550, Shimadzu, Japan) at a maximum adsorption ultraviolet wavelength of 269.0 nm and 664.0 nm, respectively. The extent of phenol or methylene blue removal was calculated by using the following equations:

$$\eta\,\% = \frac{c_0 - c_e}{c_0} \times 100\% \tag{4}$$

$$q_e = \frac{(c_0 - c_e)V}{m} \tag{5}$$

where q_e (mg/g) is the adsorption capacity at equilibrium, c_0 (mg/L) is the initial concentration of the adsorbate in solution, c_e (mg/L) is the concentration of the adsorbate in solution at equilibrium, V (L) is the volume of the solution, and m (g) is the mass of the adsorbent.

3. Results and discussion

3.1. Density

The true density of the carbon obtained from the hydrothermal carbonization of cellulose (HC) in the absence of sepiolite is 1.309 g/cm^3 (Table 1), which is lower than that of the sepiolite fibers (2.227 g/cm^3). Thus, the true density of the carbon-coated sepiolite (Table 1) is lower than that of the sepiolite. According to the measured true density of the materials in Table 1, the carbon volume fraction V_f is calculated using Eq. (1), as shown in Table 1. Due to the acid pre-treatment of the sepiolite, the carbon volume fraction of 1.2SEP/C is also higher than that of SEP/C.

The effect of the acid concentration and carbon coating on the true density of the sepiolite is shown in Table 2. The true density of the sepiolite increases initially with increasing acid concentration and then decreases with further increase of the acid concentration. The value is maximum when the acid concentration is 0.6 mol/L. Similarly, the true density of the carbon-coated acid pre-treated sepiolite initially increased and then decreased with further increase of the acid concentration, with the maximum value obtained when the acid concentration is 0.3 mol/L.

3.2. X-ray diffraction results

Fig. 1 shows the X-ray diffraction (XRD) patterns of the pristine and acid treated sepiolite. For the pristine sepiolite, XRD peaks at 2θ = 7.3°, 11.9°, 19.7° and 26.5° were observed, with the peak assignment supported by the data file JCPDS number 13-0595. The peaks at 2θ = 23.1°, 29.4°, 35.9°, 39.4°, 43.2°, 47.6° and 48.5° are due to calcite (JCPDS number 05-0586) [11]. This means that the sepiolite contained calcite impurities. The peaks at 2θ = 9.4° and 28.6° are due to talc (JCPDS number 19–0770) [16]. The calcite peak intensities decreased when the acid concentration exceeded 0.3 mol/L (0.3SEP). The calcite peaks completely disappeared when the acid concentration reached 0.6 mol/L (0.6SEP), indicating the ability of the acid to remove the calcite by dissolution. However, the sepiolite peaks remained. With the increase of the hydrochloric acid concentration up to 2.0 mol/L, the crystallinity of the sepiolite gradually decreased, as shown by the weakening and broadening of the sepiolite peaks. This is attributed to the increasing severity of the leaching of Mg^{2+} ions and the formation of silica [36]. It has been widely reported that high acidity destroys the sepiolite structure, thereby resulting in an amorphous silica-like structure and decreasing the specific surface area [15]. An intermediate acid concentration of 1.2 mol/L was thus chosen for the remainder of this investigation.

Fig. 2 shows the XRD patterns of HC, SEP/C and 1.2SEP/C. The sepiolite peaks are present in both SEP/C and 1.2SEP/C, indicating that the sepiolite remains crystalline after the acid pre-treatment and the subsequent hydrothermal treatment. No graphite 002 XRD peak (2θ = 26°) is present for HC, SEP/C or 1.2SEP/C, indicating that the carbon is amorphous in all these three materials. However, HC shows two broad XRD peaks that are centered at 2θ = 10 and 2θ = 20°. The intensities of the sepiolite XRD peaks in SEP/C and 1.2SEP/C (Fig. 2) are weaker than those of SEP (Fig. 1), due to the partial coverage of the sepiolite by the deposited carbon in SEP/C and 1.2SEP/C. This effect is as previously reported [32,37]. In addition, comparison of SEP/C and 1.2SEP/C of Fig. 2 shows that, with the acid pre-treatment, the hydrothermal process used in coating the sepiolite with carbon removes the quartz impurity from the sepiolite. In addition, comparison of SEP/C of Fig. 2 (with carbon deposition) and SEP of Fig. 1 (without carbon deposition) shows that the hydrothermal treatment removes the calcite impurity, even in the absence of the acid pre-treatment. This effect of the hydrothermal treatment is attributed to the acidic nature of the ammonium ferrous sulfate hexahydrate catalyst used in the hydrothermal process. Because of the removal of the impurities caused by the acid pre-treatment and hydrothermal process, more carbon is present in 1.2SEP/C than SEP/C, as evidenced by the weaker intensity of the diffraction peaks of sepiolite (Fig. 2).

3.3. Fourier transform infrared spectroscopy

Fig. 3 presents the FTIR spectra of SEP, 1.2SEP, SEP/C, 1.2SEP/C

Table 1
Elemental analysis (EA), specific surface area S_{BET}, total pore volume V_T (BJH), average pore diameter D (BJH), true density ρ (based on Eq. (1)) and carbon volume fraction V_f of sepiolite or carbon-coated sepiolite.

Samples	Elemental analysis (wt.%)			S_{BET} (m^2/g)	V_T (cm^3/g)	D (nm)	ρ (g/cm^3)	V_f (%)
	C	H	N					
SEP	1.27	1.24	0.07	95.86	0.101	3.172	2.054 ± 0.008	–
1.2SEP	0.67	1.87	1.17	118.13	0.129	3.192	2.227 ± 0.006	–
SEP/C	24.67	2.41	0.99	26.53	0.090	3.203	1.715 ± 0.009	45.5 ± 1.1
1.2SEP/C	31.63	3.08	2.84	33.98	0.098	3.224	1.696 ± 0.009	57.9 ± 0.9
HC	66.81	3.84	0.26	58.07	0.595	81.908	1.309 ± 0.004	–

Table 2
True density, carbon volume fraction, measured and calculated values of the phenol and methylene blue (MB) removal rate, measured and calculated values of the specific surface area of various adsorbents.

Adsorbent materials	True density (g/cm^3)	Carbon volume fraction (%))	Measured S_{BET} (m^2/g)	Calculated S_{BET} (m^2/g)	Measured phenol removal rate[a] (%)	Calculated phenol removal rate[a] (%)	Measured MB removal rate[a] (%)	Calculated MB removal rate[a] (%)
SEP	2.054 ± 0.008	–	95.86	–	5.0 ± 0.2	–	48.3 ± 0.3	–
0.3SEP	2.120 ± 0.006	–	98.57	–	5.2 ± 0.2	–	51.5 ± 0.3	–
0.6SEP	2.269 ± 0.016	–	103.89	–	5.5 ± 0.1	–	54.6 ± 0.3	–
1.0SEP	2.231 ± 0.014	–	116.78	–	5.7 ± 0.2	–	57.0 ± 0.2	–
1.2SEP	2.227 ± 0.006	–	118.13	–	6.1 ± 0.2	–	57.3 ± 0.3	–
1.4SEP	2.183 ± 0.012	–	121.87	–	5.8 ± 0.1	–	61.3 ± 0.3	–
2.0SEP	2.116 ± 0.014	–	142.14	–	6.2 ± 0.1	–	63.4 ± 0.3	–
SEP/C	1.715 ± 0.009	45.5 ± 1.1	26.53	78.67 ± 0.42	47.1 ± 0.2	39.6 ± 0.7	78.7 ± 0.1	70.1 ± 0.5
0.3SEP/C	1.738 ± 0.014	47.1 ± 1.5	27.48	78.54 ± 1.00	47.9 ± 0.2	40.7 ± 1.0	79.4 ± 0.1	72.6 ± 0.6
0.6SEP/C	1.733 ± 0.008	55.8 ± 0.9	29.81	78.32 ± 0.41	49.3 ± 0.1	47.6 ± 0.6	82.3 ± 0.1	77.8 ± 0.3
1.0SEP/C	1.719 ± 0.007	55.5 ± 0.9	32.14	84.20 ± 0.53	54.3 ± 0.2	47.5 ± 0.6	84.6 ± 0.1	78.8 ± 0.3
1.2SEP/C	1.696 ± 0.009	57.8 ± 0.9	33.98	83.44 ± 0.57	57.1 ± 0.2	49.4 ± 0.6	84.6 ± 0.1	79.8 ± 0.3
1.4SEP/C	1.689 ± 0.011	56.5 ± 1.2	35.66	85.82 ± 0.77	56.1 ± 0.1	48.3 ± 0.8	86.1 ± 0.3	81.2 ± 0.4
2.0SEP/C	1.681 ± 0.011	53.9 ± 1.3	39.67	96.83 ± 1.09	55.3 ± 0.1	46.6 ± 0.8	85.8 ± 0.2	81.1 ± 0.4
HC	1.309 ± 0.004	–	58.07	–	81.1 ± 0.2	–	96.3 ± 0.1	–
SEP + HC	–	45.5 ± 1.1	83.01	78.67 ± 0.42	42.3 ± 0.1	39.6 ± 0.7	73.8 ± 0.1	70.1 ± 0.5
1.2SEP + HC	–	57.8 ± 0.9	94.46	83.44 ± 0.57	52.9 ± 0.1	49.4 ± 0.6	82.7 ± 0.1	79.8 ± 0.3
1.2-SEP/C	1.706 ± 0.009	46.7 ± 0.9	49.71	78.21	49.4 ± 0.2	40.5 ± 0.6	80.4 ± 0.1	70.7 ± 0.5

[a] Initial phenol concentration = 5 mg/L, initial methylene blue concentration = 50 mg/L.

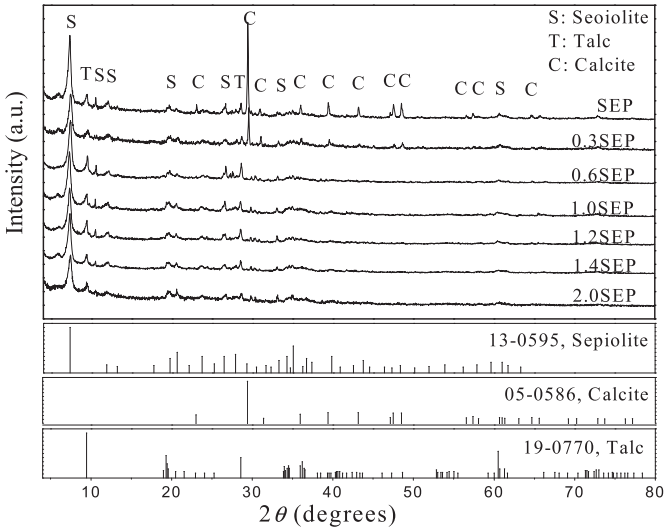

Fig. 1. XRD patterns of pristine and acid treated sepiolite. JCPDS numbers for sepiolite (13–0595), calcite (05–0586) and talc (19–0770) were used for the peak assignment.

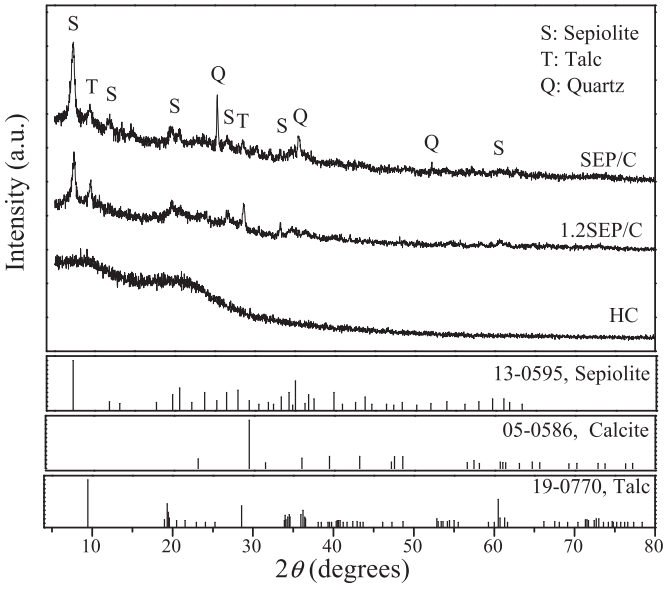

Fig. 2. XRD patterns of SEP/C, 1.2SEP/C and HC.

and HC. The peaks at 3690 and 3668 cm^{-1} correspond to the octahedral Mg–OH groups [13]. The band at 3572 cm^{-1} is attributed to the silanol groups on the surface of the sepiolite [14]. The wide band around 3408 cm^{-1} is attributed to the O–H stretching vibration of water. The peaks at 2512 and 1424 cm^{-1} are attributed to the calcite impurity [14]. The peaks at 1656 cm^{-1} are due to the OH stretching vibration of the absorbed water [23]. The bands in the range from 1200 down to 400 cm^{-1} are attributed to the characteristic peaks of sepiolite. The peaks at 1210, 1018, 980, 671 and 468 cm^{-1} are due to the Si–O and Si–O–Si stretching vibrations [36]. In particular, the peak at 980 cm^{-1} corresponds to the silanol groups [23]. After the hydrochloric acid treatment, the calcite bands at 2512 and 1424 cm^{-1}, suggesting that the calcite was removed by the acid treatment. After hydrothermal carbonization, additional adsorption peaks at 2923, 1620 and 1381 cm^{-1} appeared, corresponding to $-CH_2$, C=C and $-CH_3$, respectively. Furthermore, an additional peak at 1705 cm^{-1} that appears after the hydrothermal carbonization corresponds to the C=O vibrations from carbonyl, ester or carboxyl. The band at 1460 cm^{-1} corresponds to the C–O stretching vibrations in hydroxyl, ester or ether and the O–H bending vibrations [38]. The appearance of new bands (2923, 1705, 1620, 1460 and 1381 cm^{-1}) indicated that carbonaceous species containing organic groups were successfully formed on the surface of sepiolite [25,29,30,37]. These new bands at 2923, 1705, 1620, 1460 and 1381 cm^{-1} were also observed for HC (Fig. 3), as previously reported for the product of the hydrothermal carbonization of cellulose [38], indicating that the organic groups in SEP/C and 1.2SEP/C are caused by the deposited carbon formed by hydrothermal carbonization of cellulose. In the cases of SEP/C and 1.2SEP/C, the intensities of the peaks at 3572 and 980 cm^{-1} due to the silanol groups seem to be weaker than those of SEP and 1.2SEP. The silanol groups on the external surface of clay minerals play a key role in the interaction with biopolymers [12,22,23]. The weakening of the silanol band upon carbon deposition implies the formation of hydrogen bonds between the silanol groups in the

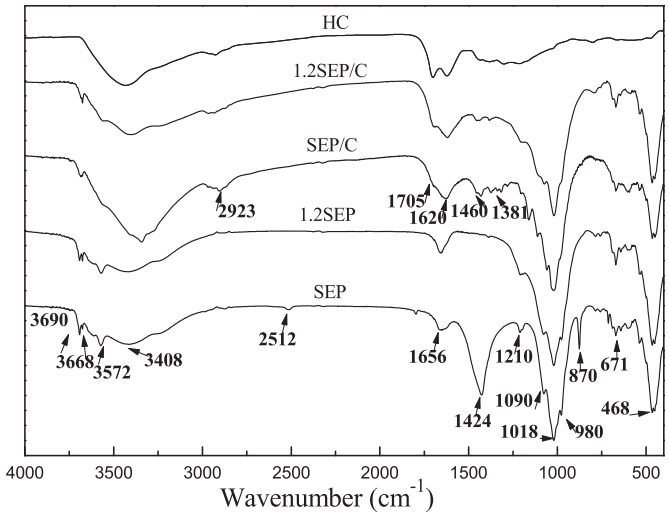

Fig. 3. FTIR spectra of SEP, 1.2SEP, SEP/C, 1.2SEP/C and HC.

sepiolite and the hydroxyls in the carbonizing cellulose [22,23,39]. In the case of HC, the characteristic peaks of sepiolite were not observed, as expected. The more pronounced nature of the peak at 1620 cm^{-1} for HC compared to the carbon-coated sepiolite (SEP/C and 1.2SEP/C) implies a higher degree of aromatization for HC than the carbon in the carbon-coated sepiolite.

3.4. Electron microscopy results

The morphology of SEP (pristine sepiolite) and 1.2SEP (acid-treated sepiolite), both without carbon deposition, is shown in Fig. 4 (a–e) (SEM) and Fig. 5 (a, b) (TEM), respectively. The SEP is in the form of fiber bundles with dispersed lumps, as previously reported [13]. The EDX data obtained at selected areas are shown in Table 3, indicating that the lumps (with a relatively high calcium content) are due to the calcite impurities. It has been previously reported that the calcite impurity regions with width 250 μm lied in the plane of the sepiolite fiber surface and covered the fiber surface [40]. The width of sepiolite bundles ranged from 500 nm to 5 μm, the length of individual fiber ranged from 1 to 10 μm and the width ranged from 10 to 30 nm. For the acid pre-treated sepiolite, the lumps disappeared (Fig. 5(b)), due to the removal of the calcite impurities. In addition, the acid-treated sepiolite bundles of width ranging from 100 to 500 nm tended to be dispersed as individual sepiolite fibers. The width and length of these individual fibers were essentially the same as those of the pristing sepiolite, indicating that the structure of the sepiolite was essentially not affected by the acid pre-treatment.

To evaluate the effect of the acid pre-treatment of the sepiolite on the hydrothermal carbon deposition, the SEM and TEM images of SEP/C and 1.2SEP/C were compared, as shown in Fig. 4 (c–d) and Fig. 5 (c, d). As mentioned above, the pristine sepiolite (SEP) was typically in the form of fiber bundles, which could not be dispersed as individual fibers by the hydrothermal process. In addition, the pristine sepiolite had calcite impurity in the form of lumps with the largest size of 0.5 μm × 2 μm, as confirmed by the EDX data (spectrum 1) in Table 3.

In the case of SEP/C, the sepiolite bundles were still observed, though hydrothermal carbon was essentially absent on the external surface of the bundles (Fig. S1(c)). Only a small amount of carbon with particle size 30–50 nm was present on the sepiolite fibers (Fig. 5(c)), as confirmed by EDX (spectrum 4) in Table 3. Due to the bundle morphology and the limited surface activity of the pristine sepiolite, the surface active sites were limited and were not adequate for receiving the carbon during the hydrothermal carbon deposition. Thus, the carbon tended to form aggregates rather than being deposited on the sepiolite surface, thus resulting in the lumps and patches (Fig. 5(c)). The sepiolite fibers did not fracture during the hydrothermal process, as previously reported [17]. In contrast to SEP, impurities such as calcite were absent in SEP/C (Figs. 2 and 3(c)), due to the acidity of the $FeSO_4(NH_4)_2SO_4 \cdot 6H_2O$ catalyst that was used in the hydrothermal carbonization of the cellulose. In addition, the hydrothermally treated cellulose aggregated and formed carbon spheres with diameter in the 50–500 nm range (Fig. S1(e), Fig. 4(e) and Fig. 5(e–f)). The formation of such spheres is as previously reported [38]. Thus, the lumps and patches in Fig. 5(c) are interpreted as aggregated carbon nanoparticles, as confirmed by the EDX data corresponding to spectrum 5 (Table 3). The carbon content of these aggregates is 86.92 wt.% (spectrum 5), which is higher than that of the carbon nanoparticles on the surface of the sepiolite (44.92 wt.% in spectrum 4).

In the case of 1.2SEP/C (Fig. S1(d), Fig. 4(d) and Fig. 5(d)), the carbon nanoparticles deposited on the sepiolite surface had size 30–150 nm. The large calcite impurity lumps present in SEP/C were absent, as confirmed by the decreased calcium content in the EDX data corresponding to spectrum 3 and spectrum 6 (Table 3). The carbon nanoparticles on the sepiolite in 1.2SEP/C are significantly larger than those for SEP/C, due to the presence of more active silanol groups on the external surface of the acid pre-treated sepiolite and the improved dispersibility of the individual fibers. The width of the individual fibers in 1.2SEP/C (ranging from 50 nm to 100 nm) was larger than those for SEP, 1.2SEP and SEP/C, due to the presence of the carbon nanoparticles on the sepiolite surface. The length of the individual fibers of SEP/C and 1.2SEP/C was similar to that of pristine sepiolite. Thus, the carbon content in 1.2SEP/C is the highest (Table 1).

The hydrothermal carbonization of cellulose tends to form carbon microspheres through a series of intermolecular dehydration and condensation reactions [38]. In this work, carbon microspheres (HC) with diameter in the 10–480 nm range were observed, as shown in Fig. S1(e), Fig. (e–f) and Fig. 5(e–f). The size of the HC particles is not uniform, having a wide size distribution (Fig. 4(f)). A large amount of reactive oxygen groups were present on the external surface of the microspheres [38]. By using a clay mineral as a template, the formation of microspheres was inhibited, so that nanocarbon was deposited on the surface of the clay mineral, as previously reported [25,29,37]. The particle size of the nanocarbon in the coating is 30–150 nm (Fig. 5(d)), which was mostly smaller than that of HC (10–480 nm). This result is in agreement with prior work, which showed that the particle size of the nanocarbon in the coating can be diminished by using a clay mineral as the template [25,29]. The hydrogen-bonding interaction between the hydroxyls groups of carboxyl in cellulose and the hydroxyl group of silanol in clay plays an important role in the hydrocarbon deposition [12,30,39,41]. In this work, the density of the silanol groups was increased by the acid pre-treatment, as explained by the reaction [36]:

$$Mg_8Si_{12}O_{30}(OH)_4(H_2O)_4 \cdot 8H_2O + 2xH^+ \rightleftharpoons Mg_{8-x}Si_{12-2x}O_{30-2x}(SiOH)_{2x}(OH)_4(H_2O)_4 \cdot 8H_2O + xMg^{2+} \quad (6)$$

In addition, more silanol groups that were present in the pristine sepiolite fibers became exposed as the sepiolite fiber bundles became dispersed as individual fibers by the acid pre-treatment [33]. Consequently, more hydroxyl groups of carboxyl in the cellulose interacted with the sepiolite, due to the increased amount of silanol groups on the sepiolite, thus resulting in the enhanced deposition of hydrothermal carbon on the sepiolite surface. In the

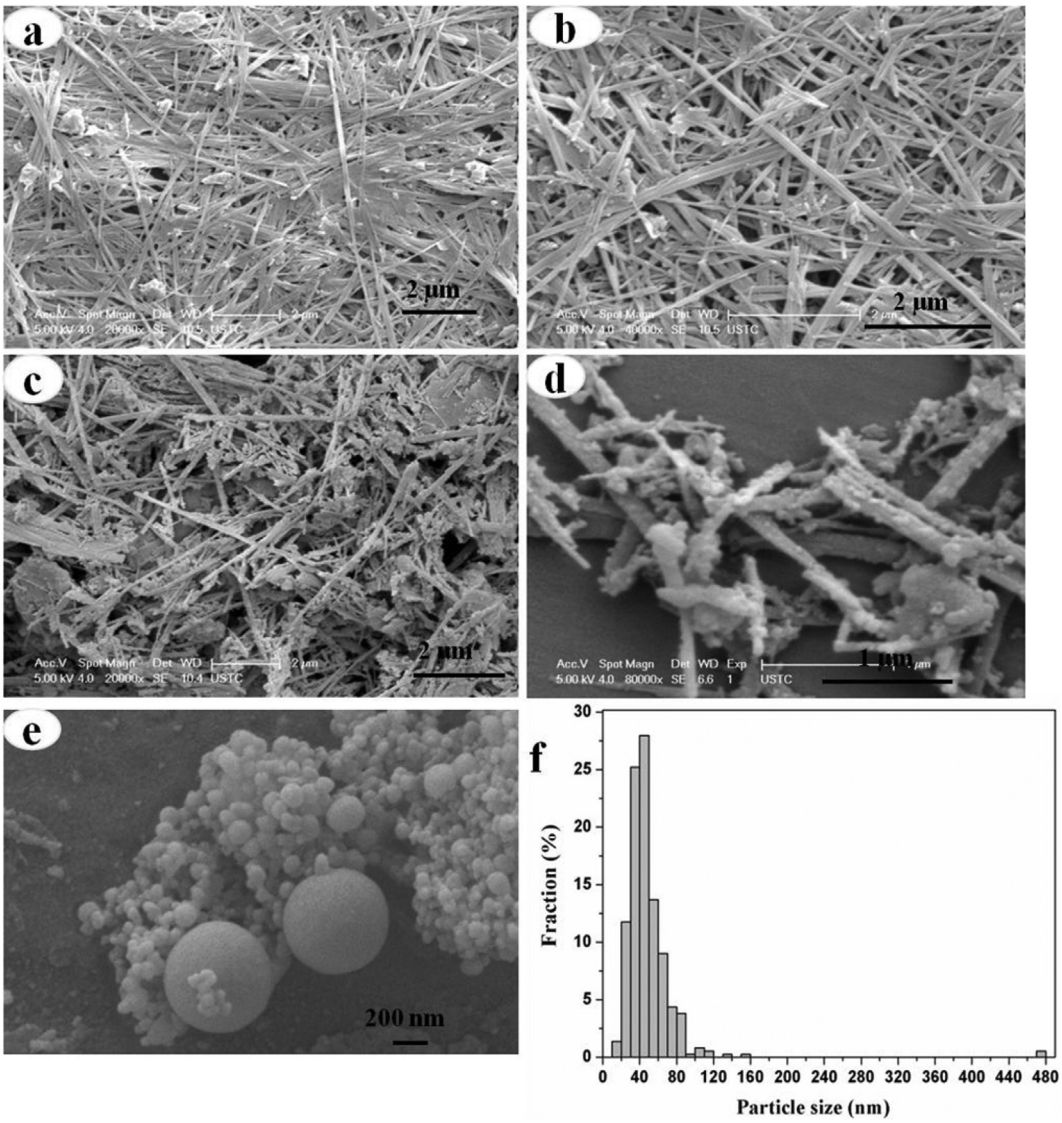

Fig. 4. SEM images of SEP (a), 1.2SEP (b), SEP/C (c), 1.2SEP/C (d), HC (e) and particle size distribution of HC (f).

prior work of some of the authors of this work, carbon-coated palygorskite was obtained by using saccharides, including glucose and cellulose, as carbon sources, without acid pre-treatment of the palygorskite [25,29]. The present work shows that, at least for the case of sepiolite, the acid pre-treatment is beneficial for the disaggregation of the fibers, in addition to promoting the deposition of nanocarbon, as confirmed by TEM (Fig. 5(d)).

3.5. Elemental analysis

Table 1 shows the elemental analysis results for the elements carbon, hydrogen and nitrogen, based on the use of the elemental analyzer. The carbon content of the pre-treated sepiolite (1.2SEP) is lower than that of the pristine sepiolite (SEP), since the carbonate impurities in the sepiolite have been removed by the hydrochloric acid used in the acid pre-treatment. The global carbon content of the carbon-coated sepiolite is increased from 24.67 to 31.63 wt.% by the acid pre-treatment of the sepiolite, as shown in Table 1. This effect of the acid pre-treatment is also indicated by the selected-area EDX results in Table 3. As shown by comparing spectra 4 and 6 (Table 3), the acid pre-treatment of the sepiolite causes the carbon content in the fiber region of the carbon-coated sepiolite to increase from 44.92 wt.% (SEP/C) to 55.42 wt.% (1.2SEP/C). For SEP/C, the patch region away from the fibers is richer in carbon than the fiber region (Table 3), because the patch region is not a part of the coating on the sepiolite fiber. The coating region is the region of interest. Table 1 shows that the carbon content is higher for HC than the carbon-coated sepiolite (whether the sepiolite has been acid pre-treated or not). This finding is also consistent with the results in Table 3.

Comparison of spectra 4 and 6 also shows that the magnesium content is decreased by the acid pre-treatment of the sepiolite prior to the carbon deposition. This suggests that the Mg^{2+} ions were leached out of the sepiolite during the acid pre-treatment. During the acid pre-treatment, the Mg^{2+} ions were extracted from the Si–O–Mg–O–Si bond by the H^{+} ions of the acid and formed Si–OH groups, in addition to the octahedral sheet of sepiolite being broken and the consequent generation of vacancies and channels, thereby causing the specific surface area and pore volume to increase [36].

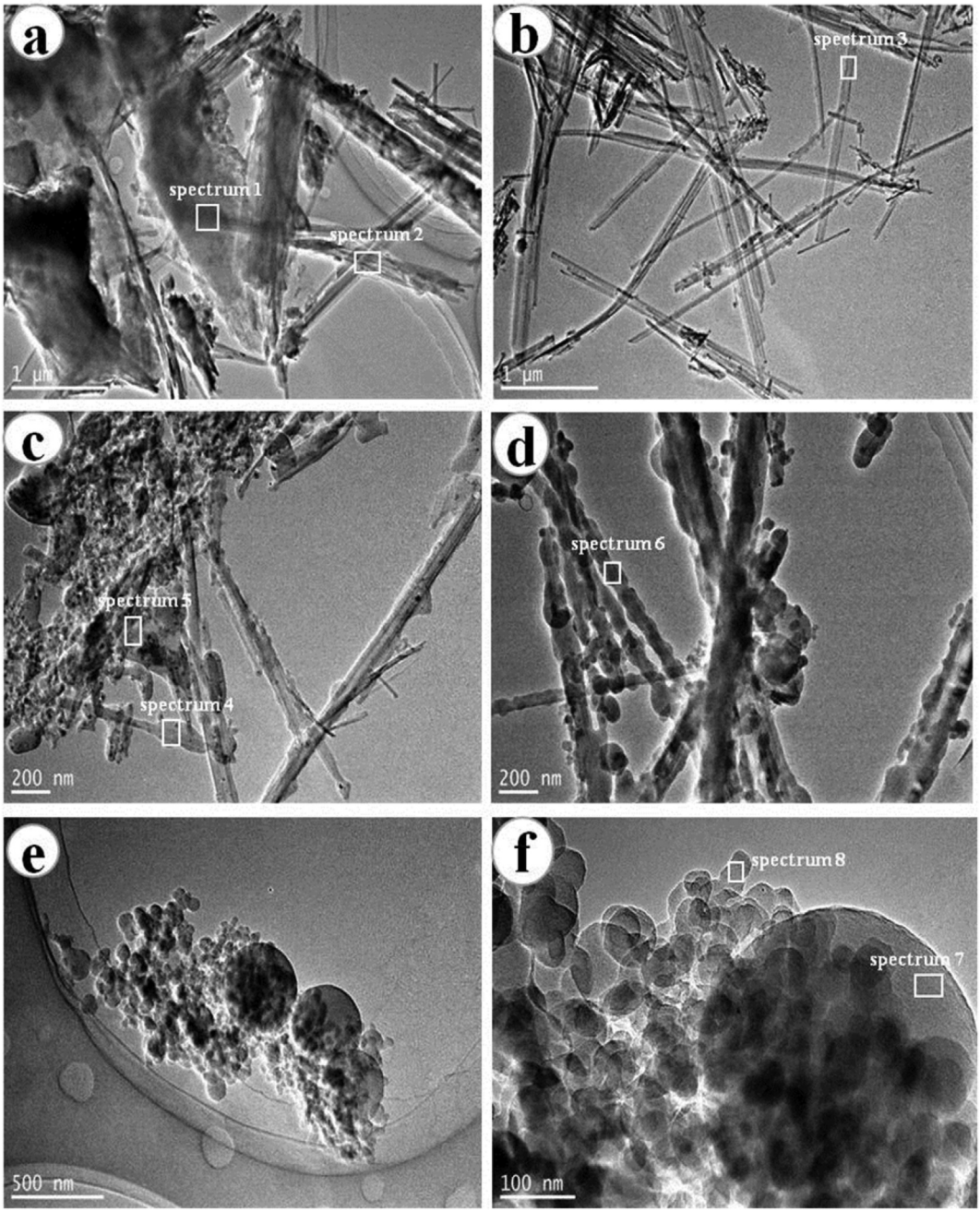

Fig. 5. TEM images of (a) SEP, (b) 1.2SEP, (c) SEP/C, (d) 1.2SEP/C, (e) HC and (f) magnified images of (e).

Comparison of spectra 4 and 6 also shows that the calcium content is decreased from 0.20 to 0.00 wt.% by the acid pre-treatment. This suggests that the calcite impurity in the sepiolite (as shown by XRD in Fig. 1) is removed by the acid pre-treatment.

3.6. Nitrogen adsorption-desorption isotherms and specific surface area

The nitrogen gas adsorption-desorption isotherms and pore structure results are shown in Fig. 6 and Table 2, respectively. Based on the IUPAC classification, SEP and 1.2SEP both exhibited the Type IV isotherm shape with the H3-type hysteresis loop [31]. The type IV shape indicates a mesoporous structure. The appearance of the H3-type hysteresis loop implies that the pores are bound by parallel plates when the relative pressure is above 0.4 [33]. Indeed, the pore size distribution indicates that the pristine and acid pre-treated sepiolite are mesoporous. With the acid pre-treatment, the total pore volume and average pore diameter slightly increase (Table 2). From Table 2, the specific surface area of sepiolite increases with increasing acid concentration. The improvement of the pore structure and surface area is attributed to the removal of calcite, better dispersion of the sepiolite fibers and the leaching of the Mg^{2+} ions from the sepiolite [16]. The leaching is supported by the decline in the magnesium content shown in Table 3.

As shown in Fig. 6(a) and (b), the carbon-coated sepiolite, whether with or without acid pre-treatment, exhibits nitrogen gas

Table 3
Energy dispersive x-ray spectroscopy (EDX, conducted with TEM) results for the selected areas labeled with the spectrum numbers in Fig. 5.

Material	Spectrum No.	Elemental content (wt.%)					
		C	O	Mg	Al	Si	Ca
SEP[a]	1	–	37.70	13.99	0.35	30.26	17.71
SEP[a]	2	–	43.96	18.27	1.06	36.58	0.13
1.2SEP[a]	3	–	52.14	17.08	0.00	30.59	0.40
SEP/C[a]	4	44.92	30.54	8.55	0.00	15.95	0.20
SEP/C[b]	5	86.92	8.71	0.15	0.00	1.34	0.18
1.2SEP/C[a]	6	55.42	27.64	3.55	0.01	13.40	0.00
HC	7	96.93	3.07	–	–	–	–
HC	8	97.85	2.15	–	–	–	–

[a] Fiber region, with high sepiolite content, as indicated by the relatively high Si content.
[b] Patch region, with low sepiolite content, as indicated by the relatively low Si content.

adsorption-desorption isotherms with a shape between those of Type II and IV and with the H3-type hysteresis loop, which suggest the dominance of mesopores. However, both the total pore volume V_T and the specific surface area are substantially decreased by the carbon deposition, whether the sepiolite has been acid treated or not (Table 2). This means that the carbon coating partly covers up the sepiolite surface, which has both high V_T and high specific surface area. In other words, the specific surface area of the carbon-coated sepiolite (both SEP/C and 1.2SEP/C) is mainly contributed by the sepiolite rather than the carbon coating. The acid treatment increases both V_T and the specific surface area to a relatively minor degree.

In this work, for the sake of comparison, cellulose in the absence of sepiolite was also hydrothermally treated. The specific surface area of the resulting carbon (HC) is 58.07 m^2/g, which is higher than that of the carbon-coated sepiolite, irrespective of the presence or absence of the acid pre-treatment of the sepiolite. The nitrogen adsorption-desorption isotherm (Fig. 6(c)) of HC exhibits a Type III shape (based on the IUPAC classification), which is characteristic of macroporous or nonporous materials [38]. The pore size distribution in Fig. 6(d) indeed indicates the macroporous structure of HC. This is consistent with the abovementioned result that the carbon coating decreases the specific surface area. The average pore width (D) is close among the four sepiolite materials (SEP, 1.2SEP, SEP/C and 1.2SEP/C) in Table 2. This indicates that the pore width is essentially not affected by the acid treatment or carbon coating.

Table 2 shows that the specific surface area S_{BET}, as measured by nitrogen adsorption, increases monotonically with increasing concentration of the HCl used in the acid treatment, whether the sepiolite has been coated with carbon or not. For the same acid concentration, S_{BET} is much lower in the presence of the carbon

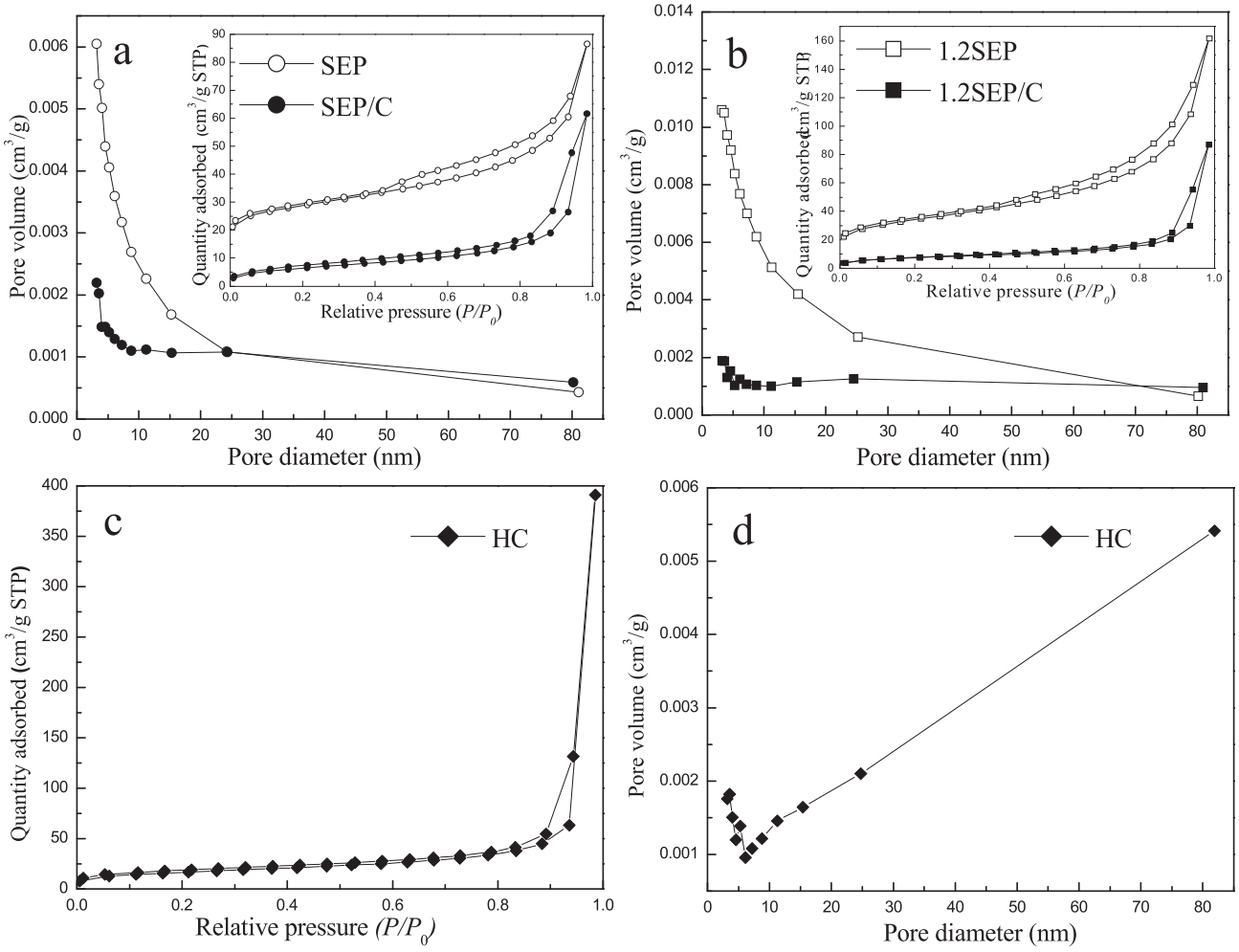

Fig. 6. Nitrogen adsorption-desorption isotherm and pore size distribution of (a) SEP and SEP/C, (b) 1.2SEP and 1.2SEP/C and (c, d) HC.

coating. In other words, the carbon coating decreases S_{BET}. The relatively low S_{BET} of the carbon-coated sepiolite is mainly due to the partial blocking of the pores of the sepiolite by the carbon particles coating the fiber, as shown by the SEM and TEM results. Also, the destruction of clay structure occurring in the hydrothermal process (Fig. S2) contributes to causing the relatively low S_{BET} of the carbon-coated sepiolite as our previous report [42]. Table 2 also shows the measured S_{BET} values of mixtures of HC and sepiolite. Comparison of the measured values of the mixtures with those of the carbon-coated sepiolite at the corresponding carbon content shows that the values are much higher for the mixtures, irrespective of the presence or absence of acid pre-treatment of the sepiolite. This difference is attributed to the partial covering, filling or blocking of the pores of the sepiolite by the carbon coating [31].

The calculated values of S_{BET} of the carbon-coated sepiolite, as obtained by using Eq. (2), are also shown in Table 2. The calculated values are lower than, but not much lower than, the measured values for the corresponding mixtures, as shown in the last two rows of Table 2. The scientific origin of this difference is presently unclear, but it may be due to the effect of the mixing process on the structure.

3.7. Phenol and methylene blue adsorption

3.7.1. Adsorption behavior

As shown in Table 2, the methylene blue removal increases monotonically with increasing HCl concentration, whether the carbon coating is present or not, with the highest removal rate provided by the highest HCl concentration of 1.4 or 2.0 mol/L. This is consistent with the monotonic increase of S_{BET} with increasing HCl concentration. On the other hand, the phenol removal rate increases with increasing HCl concentration, such that the highest removal rate occurs at an intermediate HCl concentration of 1.2 mol/L, whether the carbon coating is present or not (though the maximum at 1.2 mol/L is clearer in the presence of the carbon coating). This non-monotonic trend of the phenol removal rate is not consistent with the monotonic trend of S_{BET}. The scientific origin of this non-monotonic trend is presently not completely clear. However, it may relate to the promotion of the organophilicity by the acid treatment (with sepiolite being inherently hydrophilic) and the dependence of the HCl concentration on this effect.

For the same acid concentration, the removal rates are much higher in the presence of the carbon coating. In other words, the carbon coating increases the removal rates. This occurs despite the decrease in S_{BET} by the carbon coating, thus suggesting the importance of the surface chemistry of the carbon coating in causing the high removal rates. Based on the results of FTIR (Fig. 3) and EA (Table 1), the carbon coating is associated with $-CH_2$, $-CH_3$, C═C and C═O functional groups.

Table 2 also shows the measured phenol and methylene blue removal rates of HC and mixtures of HC and sepiolite. The values for HC are higher than those of the carbon-coated sepiolite, irrespective of the presence or absence of the acid pre-treatment of the sepiolite. Comparison of the measured values of the mixtures with those of the carbon-coated sepiolite at the corresponding carbon content shows that the values are lower for the mixtures, irrespective of the presence or absence of the acid pre-treatment of the sepiolite. This difference occurs in spite of the much higher specific surface area of the mixtures compared to the corresponding carbon-coated sepiolite. This is attributed to the much smaller value of the average pore diameter D for carbon-coated sepiolite than HC (Table 1) and to the smaller particle size for the carbon in carbon-coated sepiolite than HC (Fig. 5). This further suggests that the surface chemistry of the carbon coating differs from that of HC and is more favorable for organic adsorption than that of HC.

The calculated values of the phenol and methylene blue removal rates of carbon-coated sepiolite, as obtained by using Eq. (2), are also shown in Table 2. The calculated values are lower than, but not much lower than, the measured values of the corresponding mixtures, as shown in the last two rows of Table 2. This difference is consistent with the lower values of the calculated specific surface area compared to the corresponding measured values.

Table 2 also shows that the carbon-coated sepiolite obtained with the acid-pretreated sepiolite (1.2SEP/C) is superior to the carbon-coated sepiolite obtained without the acid pre-treatment but with acid at the same concentration (1.2 mol/L) added to the process liquid (1.2-SEP/C). The superiority pertains to the measured phenol removal rate and the measured methylene blue removal rate.

It is known that an organic acid is released to the process liquid during the hydrothermal carbonization of cellulose [29]. The acid pre-treatment of the sepiolite can improve the density of the silanol groups, which are the active sites for the hydrothermal reaction of the cellulose and further promote the carbon deposition on the sepiolite. Due to the acid release during the hydrothermal carbonization of the cellulose, the introduction of an acid to the process liquid used in the hydrothermal process tends to inhibit the hydrothermal carbonization of the cellulose. Thus, the carbon volume fraction is lower for 1.2-SEP/C than 1.2SEP/C, as shown in Table 2. Consequently, the density is slightly higher for 1.2-SEP/C. The phenol and MB removal rates for 1.2-SEP/C are both lower than those for 1.2SEP/C, although 1.2-SEP/C exhibits a higher S_{BET} value. This indicates that the adsorption is mainly contributed by the carbon that is in the form of a coating on the sepiolite.

3.7.2. Adsorption process modeling

The adsorption process was analyzed using the Langmuir and Freundlich isotherm models (Figs. S3 and S4). The Langmuir model is described by Eq. (7), where c_e is the equilibrium concentration of the adsorbate in solution (mg/L), q_e is the adsorption capacity at equilibrium (mg/g), q_m is the monolayer adsorption capacity (mg/g), K_L is the adsorption equilibrium constant (L/mg).

$$\frac{c_e}{q_e} = \frac{c_e}{q_m} + \frac{1}{q_m K_L}. \tag{7}$$

The Freundlich model is an empirical equation assuming heterogeneous adsorptive energies on an adsorbent surface. It is described by Eq. (8), where c_e is the concentration of phenol at equilibrium (mg/L), q_e is the adsorption capacity at equilibrium (mg/g), and n and K_F are empirical constants.

$$\ln q_e = \ln K_F + \frac{1}{n} \ln c_e. \tag{8}$$

The experimental data for both phenol and methylene blue adsorption fit the Langmuir model better than the Freundlich model, as shown by the higher correlation coefficient values for the former (Table 4). The Langmuir monolayer capacity q_m increases in the order SEP <1.2SEP < SEP/C < 1.2SEP/C < HC, for both phenol and methylene blue. This trend is in accordance with that of the removal rate in Table 2, further indicating the contribution of acid pre-treatment and carbon coating of the sepiolite to the adsorption enhancement. The q_m values for the absorption of phenol and methylene blue by HC are 8.59 and 147.27 mg/g, respectively, indicating that the monolayer adsorption capacity is much higher for methylene blue than phenol. With the carbon

Table 4
Parameters of the Langmuir and Freundlich models for describing the adsorption of phenol and methylene blue (MB) by various adsorbents.

Adsorbent	Adsorbate	Langmuir			Freundlich		
		q_m (mg/g)	K_L (10^{-2}L/mg)	R^2	n	K_F	R^2
SEP	Phenol	0.37	1.49	0.991	1.55	0.11	0.970
1.2SEP	Phenol	0.43	1.52	0.984	1.59	0.13	0.976
SEP/C	Phenol	4.10	1.97	0.984	1.55	0.14	0.978
1.2SEP/C	Phenol	5.26	2.65	0.993	1.54	0.21	0.950
HC	Phenol	8.59	4.05	0.981	1.69	0.50	0.978
SEP + HC[a]	Phenol	3.86	1.74	0.989	1.53	0.12	0.986
1.2SEP + HC[a]	Phenol	5.12	2.03	0.990	1.51	0.17	0.977
SEP	MB	51.41	4.56	0.986	3.34	10.22	0.751
1.2SEP	MB	63.74	5.02	0.977	3.31	12.81	0.740
SEP/C	MB	99.80	5.71	0.997	3.31	20.78	0.928
1.2SEP/C	MB	105.82	6.21	0.984	3.64	25.14	0.960
HC	MB	147.27	7.91	0.983	3.20	31.98	0.975
SEP + HC[a]	MB	97.09	4.70	0.995	3.08	17.57	0.902
1.2SEP + HC[a]	MB	102.98	5.66	0.983	3.57	23.52	0.965

[a] Mixture of the two constituents.

coating on the surface of sepiolite, the adsorption capacity increases, due to the van der Waals forces between methylene blue and the carbon coating [43]. Table 4 also shows that the mixtures of sepiolite and HC (SEP + HC and 1.2SEP + HC) exhibit lower values of q_m, K_L, n and K_F than the corresponding carbon-coated sepiolite (SEP/C and 1.2SEP/C). The Langmuir constant K_L reflects the affinity of the adsorbent for the solute. For both phenol and methylene blue, both K_L and q_m are higher for HC than the carbon-coated sepiolite, whether the sepiolite has been acid treated or not, indicating that the adsorption for these organic substances is more favorable for HC than the carbon-coated sepiolite. The high K_L value of 1.2SEP/C compared to SEP/C indicates a greater affinity for the organic substances when the sepiolite has been acid treated, as expected from the higher carbon content for the case of the acid-treated sepiolite (Tables 1 and 3). This finding is consistent with the previous report that the acid treatment of coconut shell for preparing activated carbon results in a higher monolayer adsorption capacity than coconut shell activated without the acid treatment [7]. It has been previously reported that the adsorption of phenol on a carbon layer involves the $\pi-\pi$ dispersive interaction and the electron donor-acceptor complex formation [44]. In the cases of SEP/C and 1.2SEP/C, the $\pi-\pi$ dispersive interaction occurs between the π-electrons in the aromatic rings of phenol and those in the carbon coating. The interaction between the oxygen-containing functional groups (such as the carbonyl groups) on the carbon coating and the phenol aromatic ring also enhances the adsorption capacity, due to the electron donor-acceptor mechanism [7]. Partly because of the higher content of the oxygen-containing functional groups caused by the acid pretreatment, 1.2SEP/C exhibits a higher phenol adsorption capacity than SEP/C. In contrast, the relatively low phenol adsorption ability of SEP and 1.2SEP, which have no carbon coating, is caused by the relatively weak interaction between the hydrophilic sepiolite surface and the phenol or methylene blue molecule.

In relation to the Freundlich model, the empirical constant n is higher for methylene blue than phenol, indicating that the maximum adsorption capacity of methylene blue is far higher than that of phenol, as also indicated by the Langmuir model. This is due to the electrostatic attraction between the negative charge on the sepiolite surface and the cation of the quaternary ammonium groups in methylene blue [32]. The value of n does not vary much among the various materials studied. The other empirical constant K_F varies among the various materials, such that the values relative to one another among the various materials are similar to those of K_L of the Langmuir model.

Table 5
Comparison of the monolayer adsorption capacity (q_m) for phenol and methylene blue (MB) for various clay-based adsorbents.

Adsorbents	Adsorbates	q_m	Enhancement factor	References
SEP/C	Phenol	0.37	14.22	This work
1.2SEP/C	Phenol	5.26		This work
Kaolinite	Phenol	0.52	7.40	[44]
Surfactant (HDTMA) modified kaolinite	Phenol	3.85		[44]
Clinoptilolite	Phenol	10.00	3.00	[45]
Surfactant (HDTMA) modified clinoptilolite	Phenol	30.00		[45]
Sepiolite	Phenol	12.70	12.27	[10]
SWCNTs/cal-sepiolite	Phenol	155.80		[10]
SEP	MB	51.41	2.06	This work
1.2SEP/C	MB	105.82		This work
Sepiolite	MB	79.37	1.62	[46]
Sonicated sepiolite	MB	128.21		[46]
Palygorskite	MB	48.39	1.61	[47]
Calcined Palygorskite	MB	78.11		[47]
Zeolite	MB	8.67	1.81	[48]
Surfactant(SDBS) modified zeolite	MB	15.68		[48]

Notes: The enhancement factor refers to the factor of improvement of the adsorption capacity of the modified adsorbent in comparison with that of the corresponding unmodified adsorbent.

3.7.3. Comparison of various adsorbents

A comparison of the monolayer adsorption capacity (q_m) of various clay-based adsorbents, including those of this work and those of prior work [10,44–48], is shown in Table 5. The q_m values for different adsorbents are quite different for the same adsorbate. The q_m values for phenol and methylene blue are in the range 0.37–155.80 and 8.67–128.21 mg/g, respectively. The modification methods used in preparing these adsorbents include acid, heat and sonic treatments. They are effective for improving the adsorption capacity of organic substances on clay minerals because of the effect on the surface area and surface chemistry of the clays. The enhancement factor, which refers to the factor by which q_m is increased, is also shown to facilitate the comparison of the effectiveness of the modification methods. The enhancement factor for phenol ranges from 3.00 to 12.27 and that for methylene blue ranges from 1.61 to 1.81 [45–49]. Among these adsorbents, single-walled carbon nanotubes (SWCNTs) were used to coat sepiolite by chemical vapor deposition in order to improve the adsorption capacity of the sepiolite [10]. The phenol adsorption capacity is thus enhanced by a factor of 12.27, due to the $\pi-\pi$ dispersive interaction and electron donor-acceptor complex formation between phenol and carbon. The methods of Table 5 are efficient for the enhancement of the adsorption ability of clay minerals, but their costs are relatively high and the processes involved are quite complex. In our study, the combination of acid pre-treatment and hydrothermal carbon deposition provides a low-cost and effective method of modifying sepiolite that gives the highest values of the enhancement factor in Table 5, namely 14.22 and 2.06 (relative to pristine sepiolite) for phenol and methylene blue, respectively. The difference in the enhancement factor between phenol and methylene blue reflects the difference in the effect of the carbon coating on the adsorption process. The carbon coating has a stronger effect for phenol adsorption than methylene blue adsorption. For the same pristine sepiolite adsorbent, the monolayer adsorption capacity q_m for phenol is low (0.37 mg/g), while that for cationic methylene blue is high (51.41 mg/g) (Table 4), due to electrostatic attraction of ions provided by the negatively charged sepiolite. Consequently, the enhancement factor of methylene blue is far lower than that of phenol (Table 5).

The commercial cost estimates for some of the adsorbents are compared in Table 6. The Langmuir monolayer capacity q_m increases in the order SEP <1.2SEP/C < HC, for both phenol and methylene blue, as shown in Table 4. The carbon nanotube or 3D foam of graphene are structurally attractive materials that have received considerable prior attention. The 3D foam of graphene is very expensive, with its price being $1463/g. Commercial carbon nanotube was evaluated in this work in terms of its adsorption ability. For the adsorption of phenol and MB adsorption on carbon nanotube, the organic removal rates were 73.2% for phenol and 86.5% for MB under the same adsorption conditions as Table 2. The values are both higher than those for carbon-coated sepiolite. In spite of the cost increase due to the acid treatment and carbon coating of the sepiolite, the modified sepiolite is still less expensive than HC, activated carbon, carbon nanotube and graphene. Also, the compressive strength of carbon including graphene is not higher than that of clay-supported carbon [31,50,51], indicating the attraction of hydrothermal-carbon-nanoparticle-coated sepiolite for use as a block adsorbent in wastewater treatment. Furthermore, the carbon nanoparticles coating the sepiolite are accompanied by C=C, $-CH_2$, $-CH_3$ and C=O groups (Fig. 3), which are expected to enable the modified sepiolite to be effective for the adsorption of a variety of organic specieces. All of the above consideration suggest that hydrothermal-carbon-nanoparticle-coated sepiolite can serve as a low-cost adsorbent for adsorbing organic substances that include phenol and methylene blue.

Table 6
Estimated cost of selected adsorbents.

Adsorbent	Preparation conditions	Price (US $/kg)
SEP	Natural	~0.21
HC	220 °C, 48 h, this work	~2.23
1.2SEP/C	220 °C, 48 h, this work	~1.56
Commercial activated carbon	300–1000 °C [7–9]	1.37–20.00

4. Conclusions

The organophilicity enhancement of sepiolite is achieved in this work by depositing hydrothermal carbon in the form of carbon nanoparticles (nanocarbon) on sepiolite. The deposition results in the enhancement of the adsorption capacity of sepiolite for organic substances, namely phenol and methylene blue. The acid pre-treatment of the sepiolite enhances the amount of deposited carbon, thereby improving the effectiveness for adsorbing organic substances, with the acid pre-treatment increasing the fraction of phenol removed by adsorption from 47.1% to 57.1% and increasing the maximum phenol adsorption capacity from 4.10 to 5.26 mg/g. A hydrochloric acid concentration of 1.2 mol/L is optimum for maximizing the amount of carbon deposited. This maximum is 57.8 vol% carbon compared to 45.5 vol% in the absence of the acid pre-treatment. The acid pre-treatment increases the specific surface area of the carbon-coated sepiolite from 26.53 to 33.98 m^2/g, as enabled by the increase of the density of the silanol groups. Compared to sepiolite, or a mixture of sepiolite and hydrothermal carbon, the carbon-coated sepiolite exhibits better adsorption capacity at a lower cost.

The pristine sepiolite was pre-treated by hydrochloric acid solutions at different concentrations. The calcite impurities were removed by the acid treatment. The crystal structures and fibrous morphology are not affected by the acid pre-treatment. The acid pre-treatment is beneficial for the increase of the specific surface area and enhancing the adsorption properties of the sepiolite. More importantly, the acid pre-treatment of sepiolite promotes the deposition of nanocarbon on the sepiolite, due to the enhanced density of the silanol groups provided by the acid pre-treatment. The nanocarbon is formed by the hydrothermal carbonization of cellulose. The hydrogen bonding interactions between the hydroxyl groups of the carboxyl from the carbonizing cellulose and the hydroxyl group of the silanol in the sepiolite directly lead to the promoted deposition of carbon on the sepiolite. The carbon content increased from 24.67 wt.% for the carbon-coated sepiolite without acid pre-treatment to 31.63 wt.% for the carbon-coated sepiolite with acid pre-treatment, while the carbon volume fraction increased from 45.5% to 57.8%. The nanocarbon with particle diameter ranging from 30 to 150 nm was deposited on the sepiolite surface. This acid pre-treatment method may be applied to other clay minerals (such as halloysite and palygorskite) for obtaining a hydrothermal nanocarbon coating.

Compared to the pristine sepiolite, the pore volume and specific surface area of the carbon-coated sepiolite are smaller, while the adsorption capacity for phenol is higher, due to the deposited nanocarbon being accompanied by C=C, $-CH_2$, $-CH_3$ and C=O groups. The acid concentration of 1.2 mol/L is optimum for maximizing the organic adsorption. The phenol and methylene blue adsorption capacity for the carbon-coated sepiolite obtained with the acid pre-treatment of the sepiolite was 5.26 mg/g and 105.82 mg/g, respectively, i.e.,14.22-fold and 2.06-fold, respectively, higher than the values for the pristine sepiolite (0.37 mg/g and

51.41 mg/g). The corresponding removal rates of phenol and methylene blue are 57.1% and 84.6%, respectively. The phenol and methylene blue adsorption on the pristine sepiolite and carbon-coated sepiolite conformed to the Langmuir model. Compared to a mixture of pristine sepiolite and hydrothermal carbon with the same constituent proportions, the carbon-coated sepiolite also exhibits a higher adsorption capacity. Compared to the carbon-coated sepiolite obtained without the acid pre-treatment of the sepiolite but with the acid at the same concentration added to the process liquid during the hydrothermal carbonization, the carbon-coated sepiolite obtained with the acid pre-treatment of the sepiolite exhibits a higher adsorption capacity.

Acknowledgments

This work was financially supported in part by the National Natural Science Foundation of China (No. 51002042 and No. 40902020), the Fundamental Research Funds for the Central Universities (No. 2013HGQC0015), Scientific Research Foundation for the Returned Scholars from Ministry of Education of China (No. 2013JYLH0774) and Project from Ministry of Science and Technology of Anhui Province (No. J2014AKKG0002).

Appendix A. Supplementary data

Supplementary data related to this article can be found at http://dx.doi.org/10.1016/j.carbon.2017.07.063.

References

[1] R.I. Yousef, B. El-Eswed, A.A.H. Al-Muhtaseb, Adsorption characteristics of natural zeolites as solid adsorbents for phenol removal from aqueous solutions: kinetics, mechanism, and thermodynamics studies, Chem. Eng. J. 171 (3) (2011) 1143–1149.
[2] Y. Yavuz, A. Savas Koparal, Bakir Ögütveren Ü. Phenol removal through chemical oxidation using fenton reagent, Chem. Eng. Technol. 30 (5) (2007) 583–586.
[3] Y. Wang, H. Sun, X. Duan, H.M. Ang, M.O. Tadé, S. Wang, A new magnetic nano zero-valent iron encapsulated in carbon spheres for oxidative degradation of phenol, Appl. Catal. B 172–173 (2015) 73–81.
[4] W. Oh, S. Lua, Z. Dong, T.T. Lim, Performance of magnetic activated carbon composite as peroxymonosulfate activator and regenerable adsorbent via sulfate radical-mediated oxidation processes, J. Hazard. Mater. 284 (2015) 1–9.
[5] H. Liang, H. Sun, A. Patel, P. Shukla, Z.H. Zhu, S. Wang, Excellent performance of mesoporous Co_3O_4-MnO_2 nanoparticles in heterogeneous activation of peroxymonosulfate for phenol degradation in aqueous solutions, Appl. Catal. B 127 (2012) 330–335.
[6] A. Babuponnusami, K. Muthukumar, A review on Fenton and improvements to the Fenton process for wastewater treatment, J. Env. Chem. Eng. 2 (1) (2014) 557–572.
[7] K.P. Singh, A. Malik, S. Sinha, P. Ojha, Liquid-phase adsorption of phenols using activated carbons derived from agricultural waste material, J. Hazard. Mater. 150 (3) (2008) 626–641.
[8] K. Gergova, S. Eser, Effects of activation method on the pore structure of activated carbons from apricot stones, Carbon 34 (1996) 879–888.
[9] P. Hadi, M. Xu, C. Ning, C. Sze Ki Lin, G. McKay, A critical review on preparation, characterization and utilization of sludge-derived activated carbons for wastewater treatment, Chem. Eng. J. 260 (2015) 895–906.
[10] J. Nie, Q. Zhang, M. Zhao, J. Huang, Q. Wen, Y. Cui, et al., Synthesis of high quality single-walled carbon nanotubes on natural sepiolite and their use for phenol absorption, Carbon 49 (2011) 1568–1580.
[11] S. Lazarević, I. Janković-Častvan, D. Jovanović, S. Milonjić, D. Janaćković, R. Petrović, Adsorption of Pb^{2+}, Cd^{2+} and Sr^{2+} ions onto natural and acid-activated sepiolite, Appl. Clay Sci. 37 (2007) 47–57.
[12] E. Ruiz-Hitzky, M. Darder, F.M. Fernandes, B. Wicklein, A.C.S. Alcântara, P. Aranda, Fibrous clays based bionanocomposites, Prog. Polym. Sci. 38 (10–11) (2013) 1392–1414.
[13] S. Letaief, S. Grant, C. Detellier, Phenol acetylation under mild conditions catalyzed by gold nanoparticles supported on functional pre-acidified sepiolite, Appl. Clay Sci. 53 (2) (2011) 236–243.
[14] Y. Qiu, S. Yu, Y. Song, Q. Wang, S. Zhong, W. Tian, Investigation of solution chemistry effects on sorption behavior of Sr(II) on sepiolite fibers, J. Mol. Liq. 180 (2013) 244–251.
[15] J.L. Valentín, M.A. López-Manchado, A. Rodríguez, P. Posadas, L. Ibarra, Novel anhydrous unfolded structure by heating of acid pre-treated sepiolite, Appl. Clay Sci. 36 (4) (2007) 245–255.
[16] A. Miura, K. Nakazawa, T. Takei, N. Kumada, N. Kinomura, R. Ohki, et al., Acid-, base-, and heat-induced degradation behavior of Chinese sepiolite, Ceram. Int. 38 (6) (2012) 4677–4684.
[17] E. Duan, J. Han, Y. Song, Y. Guan, W. Zhao, B. Yang, et al., Adsorption of styrene on the hydrothermal-modified sepiolite, Mater. Lett. 111 (2013) 150–153.
[18] A.S. Özcan, Gök Ö, Structural characterization of dodecyltrimethylammonium (DTMA) bromide modified sepiolite and its adsorption isotherm studies, J. Mol. Struct. 1007 (2012) 36–44.
[19] N. Frini-Srasra, E. Srasra, Acid treatment of south Tunisian palygorskite: removal of Cd(II) from aqueous and phosphoric acid solutions, Desalination 250 (1) (2010) 26–34.
[20] A. Zhang, L. Pan, H. Zhang, S. Liu, Y. Ye, M. Xia, et al., Effects of acid treatment on the physico-chemical and pore characteristics of halloysite, Colloids Surfaces A 396 (2012) 182–188.
[21] M. Myriam, M. Suárez, J.M. Martín-Pozas, Structure and textural modifications of palygorsite and sepiolite under acid treatment, Clays Clay Miner. 46 (3) (1998) 225–231.
[22] M. Dader, M. López-Blanco, P. Aranda, A.J. Aznar, J. Bravo, E. Ruiz-Hitzky, Microfibrous chitosan-sepiolite nanocomposites, Chem. Mater 18 (2006) 1602–1610.
[23] M. Soheilmoghaddam, M.U. Wahit, A.A. Yussuf, M.A. Al-Saleh, W.T. Whye, Characterization of bio regenerated cellulose_sepiolite nanocomposite films prepared via ionic liquid, Polym. Test. 33 (2014) 121–130.
[24] F. Chivrac, E. Pollet, M. Schmutz, L. Avérous, Starch nano-biocomposites based on needle-like sepiolite clays, Carbohydr. Polym. 80 (1) (2010) 145–153.
[25] X. Wu, W. Zhu, X. Zhang, T. Chen, R.L. Frost, Catalytic deposition of nano-carbon onto palygorskite and its adsorption of phenol, Appl. Clay Sci. 52 (4) (2011) 400–406.
[26] D. Liu, P. Yuan, D. Tan, H. Liu, M. Fan, A. Yuan, et al., Effects of inherent/enhanced solid acidity and morphology of diatomite templates on the synthesis and porosity of hierarchically porous carbon, Langmuir 26 (24) (2010) 18624–18627.
[27] Y. Seo, K. Kim, Y. Jung, R. Ryoo, Synthesis of mesoporous carbons using silica templates impregnated with mineral acids, Microporous Mesoporous Mater 207 (2015) 156–162.
[28] A.B. Albadarin, J. Mo, Y. Glocheux, S. Allen, G. Walker, C. Mangwandi, Preliminary investigation of mixed adsorbents for the removal of copper and methylene blue from aqueous solutions, Chem. Eng. J. 255 (2014) 525–534.
[29] X. Wu, P. Gao, X. Zhang, G. Jin, Y. Xu, Y. Wu, Synthesis of clay/carbon adsorbent through hydrothermal carbonization of cellulose on palygorskite, Appl. Clay Sci. 95 (2014) 60–66.
[30] X. Wu, C. Liu, H. Qi, X. Zhang, J. Dai, Q. Zhang, et al., Synthesis and adsorption properties of halloysite/carbon nanocomposites and halloysite-derived carbon nanotubes, Appl. Clay Sci. 119 (2016) 284–293.
[31] X. Zhang, L. Cheng, X. Wu, Y. Tang, Y. Wu, Activated carbon coated palygorskite as adsorbent by activation and its adsorption for methylene blue, J. Environ. Sci. 33 (2015) 97–105.
[32] X. Wu, Y. Xu, X. Zhang, Y. Wu, P. Gao, Adsorption of low-concentration methylene blue onto a palygorskite/carbon composite, New Carbon Mater 30 (1) (2015) 71–78.
[33] M. Suárez, E. García-Romero, Variability of the surface properties of sepiolite, Appl. Clay Sci. 67–68 (2012) 72–82.
[34] M.S. Barrios, F.L.V. González, M.A.V. Rodríguez, J.M.M. Pozas, Acid activation of a palygorskite with HCl Development of physico-chemical, textural and surface properties, Appl. Clay Sci. 10 (1995) 247–258.
[35] A. Wang, X. Gao, R.F. Giese, D.D.L. Chung, A ceramic–carbon hybrid as a high-temperature structural monolith and reinforcing filler and binder for carbon/carbon composites, Carbon 59 (2013) 76–92.
[36] A. Esteban-Cubillo, R. Pina-Zapardiel, J.S. Moya, M.F. Barba, C. Pecharromán, The role of magnesium on the stability of crystalline sepiolite structure, J. Eur. Ceram. Soc. 28 (9) (2008) 1763–1768.
[37] L. Chen, H. Liang, Y. Lu, C. Cui, S. Yu, Synthesis of an attapulgite clay@carbon nanocomposite adsorbent by a hydrothermal carbonization process and their application in the removal of toxic metal ions from water, Langmuir 27 (2011) 8998–9004.
[38] M. Sevilla, A.B. Fuertes, The production of carbon materials by hydrothermal carbonization of cellulose, Carbon 47 (9) (2009) 2281–2289.
[39] L. Wu, D. Tong, S. Li, C. Lin, H. Yang, Z. Zhong, et al., Insight into formation of montmorillonite-hydrochar nanocomposite under hydrothermal conditions, Appl. Clay Sci. 119 (2016) 116–125.
[40] L. Lescano, L. Castillo, S. Marfil, S. Barbosa, P. Maiza, Alternative methodologies for sepiolite defibering, Appl. Clay Sci. 95 (2014) 378–382.
[41] L. Wu, D. Tong, L. Zhao, W. Yu, C. Zhou, H. Wang, Fourier transform infrared spectroscopy analysis for hydrothermal transformation of microcrystalline cellulose on montmorillonite, Appl. Clay Sci. 95 (2014) 74–82.
[42] X. Wu, C. Liu, L. Zhang, X. Zhang, L. Cheng, Effect of hydrothermal treatment on structural character of palygorskite and adsorption efficiency for methylen blue, Adv. Mater. Res. 726–731 (2013) 560–564.
[43] E.I. El-Shafey, S.N.F. Ali, S. Al-Busafi, H.A.J. Al-Lawati, Preparation and characterization of surface functionalized activated carbons from date palm leaflets and application for methylene blue removal, J. Env. Chem. Eng. 4 (3) (2016) 2713–2724.
[44] Q. Liu, T. Zheng, P. Wang, J. Jiang, N. Li, Adsorption isotherm, kinetic and

mechanism studies of some substituted phenols on activated carbon fibers, Chem. Eng. J. 157 (2–3) (2010) 348–356.
[45] U.F. Alkaram, A.A. Mukhlis, A.H. Al-Dujaili, The removal of phenol from aqueous solutions by adsorption using surfactant-modified bentonite and kaolinite, J. Hazard. Mater 169 (1–3) (2009) 324–332.
[46] H. Wang, H. Huang, J. Jiang, The effect of metal cations on phenol adsorption by hexadecyl-trimethyl-ammonium bromide (hdtma) modified clinoptilolite (Ct.), Sep. Purif. Technol. 80 (3) (2011) 658–662.
[47] Şener S. Küncek İ, Adsorption of methylene blue onto sonicated sepiolite from aqueous solutions, Ultrason. Sonochem 17 (1) (2010) 250–257.
[48] H. Chen, J. Zhao, A. Zhong, Y. Jin, Removal capacity and adsorption mechanism of heat-treated palygorskite clay for methylene blue, Chem. Eng. J. 174 (1) (2011) 143–150.
[49] X. Jin, M. Jiang, X. Shan, Z. Pei, Z. Chen, Adsorption of methylene blue and orange II onto unmodified and surfactant-modified zeolite, J. Colloid Interface Sci. 328 (2) (2008) 243–247.
[50] Jinhui Li, Weixin Li, Wangping Huang, Guoping Zhang, Rong Sun, Ching-Ping Wong, Fabrication of highly reinforced and compressible graphene/carbon nanotube hybrid foams via a facile self-assembly process for application as strain sensors and beyond, J. Mater. Chem. C 5 (2017) 2723–2730.
[51] L.V. Jinlong, Yang Meng, Ken Suzuki, Hideo Miura, Fabrication of 3D graphene foam for a highly conducting electrode, Mater. Lett. 196 (2017) 369–372.